J. Fluid Mech. (1976), *vol.* 76, *part* 2, *pp.* 259–272
Printed in Great Britain

Internal wave reflexion from a sinusoidally corrugated surface

By R. P. MIED AND J. P. DUGAN
Ocean Sciences Division, Naval Research Laboratory, Washington, D.C. 20375

(Received 31 August 1975)

The reflexion of an internal gravity wave with stream function

$$\psi = \exp\{i(kx + lz - \omega t)\}$$

from a corrugated surface of the form $z = a\cos px$ is investigated using an extension of Rayleigh's method for an inviscid non-diffusive fluid. It is found that the method converges for many wall slopes ap and incoming-wave phase propagation incidence angles $\theta = \tan^{-1} l/k$ but that the appropriate series solution is only asymptotic in other cases. The accuracy of the calculations is assured by requiring that the solution satisfy the boundary condition at the wall using a least-squares error minimization technique. The accuracy is then verified through the conservation of energy flux. It is found that, as the surface slope is increased for constant θ, less energy appears in specular reflexions and more is either back-scattered or redistributed into other forward-scattered modes. As the horizontal internal wavelength is decreased to become comparable to the corrugation wavelength of the wall, substantially less energy appears in specular reflexion, but of the order of 95 % of the incoming energy is specularly reflected for $30° < \theta < 60°$ when the two wavelengths are equal. In contrast to this, it is found that the general level of the ratio of back-scattered to forward-scattered energy is reduced by $O(10^{-3})$ to $O(10^{-2})$ as the incident horizontal internal wavelength becomes smaller than the corrugation wavelength. The results are compared with the linear theory of Baines (1971); agreement is good for forward-scattered energy and excellent for the back-scattered flux when $p \geqslant k$.

1. Introduction

Internal wave propagation in the ocean is of great interest to the oceanographer because these waves provide a mechanism whereby energy and momentum may be vertically transported over a depth of several kilometres. For example, lee waves generated by the motion of the tides over a rough bottom (Bell 1975; Lee & Beardsley 1974) can propagate upwards towards the surface. After impinging upon the thermocline, they may pass virtually unaltered through it only to be totally reflected back downwards by the free surface, or they may be almost totally reflected by the thermocline. This latter phenomenon is seen to be the case whenever the vertical wavenumber is the order of (or larger than) the magnitude of the scale height of the thermocline (Mied & Dugan 1974).

Under similar circumstances, a region of horizontal current shear can also reflect a substantial amount of wave energy back down towards its region of origin (Mied & Dugan 1975).

On the other hand, internal gravity waves generated in the vicinity of the surface – by the action of the wind stress, say – can propagate away from the free surface into the deep ocean. There they can be seen to be reflected by the bottom topography, but with results that are of a vastly different qualitative nature. By employing the method of characteristics and the appropriate radiation condition, Baines (1971) examines the properties of waves reflected from solid, rough surfaces. Specifically, these properties are:

(i) Back-reflexion. In addition to the forward-scattered waves present in the case of thermocline/current-shear reflexion, there can exist back-scattered waves which propagate energy back along the characteristic on which the incoming waves transport energy.

(ii) Change of horizontal scattered wavenumber. Unlike thermocline/shear reflexions, which keep invariant the horizontal wavenumber of incident and scattered waves, topographic reflexions alter the horizontal wavenumber of the forward- and back-scattered waves.

The direction of travel of the scattered modes is dependent only upon the wave frequency, which is an invariant in this linearized problem. Hence the above results mirror the fact that the scattered wavenumbers are algebraic combinations of the incident and topographical wavenumbers.

In the present paper, we seek a solution to the problem posed when plane internal waves with stream function

$$\psi = \exp\{i(|k|\,x + |l|\,z - \omega t)\}$$

in a fluid of constant Brunt–Väisälä frequency reflect from a rough surface of the form

$$z = a\cos px.$$

Making the Boussinesq approximation, assuming only small amplitude internal waves, and employing an extension of Rayleigh's (1945) method to permit oblique wave incidence in a non-acoustic application, we have solved this problem numerically for arbitrary wall slopes and a variety of ratios of l/k and p/k. The wave field is comprised of the incident wave and an infinite set of reflected waves. Much of the reflected wave energy may be carried off in a specular mode,† but some of it propagates in higher-order modes, both in the forward direction and back towards the direction of the source. The functional representation of these scattered waves is an infinite series, and the relative amplitudes of the unknown coefficients are obtained by minimizing the error incurred in satisfying the boundary condition at many collocation points along the wavy wall.

The convergence of the series solution is a matter of concern since related series solutions in acoustic and electromagnetic wave reflexion have failed to converge in some circumstances. As a check on the series convergence rate, an independent error criterion, namely the accuracy to which the energy in the scattered field is conserved, is monitored.

† The specularly reflected wave has wavenumber $(|k|, -|l|)$.

2. Theory

The Boussinesq equation governing the stream function for small amplitude wave motion in an inviscid non-diffusive fluid is given by Phillips (1966):

$$\partial^2(\nabla^2\psi)/\partial t^2 + N^2(z)\,\partial^2\psi/\partial x^2 = 0. \tag{1}$$

Here, t is time, ∇^2 is the Laplacian in the (x, z) co-ordinate system, ψ is the stream function related to the velocity in these co-ordinates by $\mathbf{u} = (u, v) = (-\psi_z, \psi_x)$, and the Brunt–Väisälä frequency $N(z)$ is given by

$$N^2(z) = (-g/\rho)\,(d\rho/dz), \tag{2}$$

where $\rho = \rho(z)$ is the density of the rest state. The plane wave

$$\psi = \exp\{i(|k|\,x + |l|\,z - \omega t)\}$$

can be seen to satisfy (1) in the case of constant N^2 provided

$$|k|/(k^2+l^2)^{\frac{1}{2}} = \omega/N, \tag{3}$$

which is the dispersion relation for the wave.

The group velocity is given by

$$\mathbf{c}_g = \left[\frac{N\,\mathrm{sgn}\,(k)}{(k^2+l^2)^{\frac{1}{2}}} - \frac{Nk\,|k|}{(k^2+l^2)^{\frac{3}{2}}},\ \frac{-N\,|k|\,l}{(k^2+l^2)^{\frac{3}{2}}}\right]. \tag{4}$$

As indicated by the dispersion relation (3), these waves are anisotropic, their frequency being dependent upon the direction of propagation. In view of the linearity of (1), any reflexion of these waves from a stationary boundary – just so long as a linear boundary condition is used – must preserve the frequency of the incoming waves. Thus, from (3), we see that phase propagation of the reflected waves is constrained to be along the two directions which are at angles

$$\theta = \begin{cases} -\cos^{-1}[|k|/(k^2+l^2)^{\frac{1}{2}}] & (5a) \\ \pi + \cos^{-1}[|k|/(k^2+l^2)^{\frac{1}{2}}] & (5b) \end{cases}$$

to the $+x$ axis. These correspond to the directions of forward- and back-scattered phase propagation, which must be represented in the stream function for the scattered wave field. Accordingly, we express the stream function ψ as the sum of an incoming wave and scattered waves:

$$\psi = \psi_{\mathrm{in}} + \psi_{\mathrm{sc}}. \tag{6}$$

Clearly, ψ_{in} must satisfy the equation independently of the scattered wave field; hence we take

$$\psi_{\mathrm{in}} = \exp\{i(kx + lz - \omega t)\} \quad (k,\, l \geqslant 0), \tag{7}$$

and put

$$\psi_{\mathrm{sc}} = \sum_{n=-\infty}^{+\infty} A_n \exp\{i(k_n x - |l_n|\,z - \omega t)\}, \tag{8}$$

where the k_n and l_n are unspecified as yet. In view of the equation (4) for the group velocity, (7) and (8) are consistent with the radiation condition that ψ_{in} represents incoming energy, while ψ_{sc} contains all of the energy propagating away from the reflecting surface. If this reflecting surface is periodic, $z = a\cos px$ say, then we should expect the scattering coefficient

$$R(x, z) = \psi_{\mathrm{sc}}/\psi_{\mathrm{in}}$$

to have period $2\pi/p$ also: $\quad R(x, z) = R(x + 2\pi/p, z)$.

From (7) and (8), we see that this requires

$$k_n - k = np, \tag{9}$$

where n is an integer; and, because the frequency is conserved, the dispersion relation (3) constrains the magnitude of the ratio of reflected wavenumbers to be constant:

$$k/l = |k_n/l_n|. \tag{10}$$

The scattered horizontal wavenumbers k_n are thus algebraic combinations of the wall wavenumber p and the incoming horizontal wavenumber k. More significant, however, (9) determines along which of the two possible directions the scattered waves will propagate. For all modes with $n > -k/p$, the waves are forward-scattered and the direction of phase propagation is given by (5*a*). If on the other hand $n < -k/p$, the reflected waves are back-scattered, the propagation direction being given by (5*b*). The case $n = -k/p$ corresponds to a vertically propagating wave and is discussed in §4.

If these waves impinge upon a solid impermeable boundary, the normal fluid velocity vanishes there, so that for a surface specified by

$$z = F(x),$$

or

$$\eta = z - F(x) = 0,$$

the boundary condition is given by

$$[d\eta/dt]_{z=F(x)} = 0. \tag{11}$$

In terms of the stream function, the boundary condition is

$$[\psi_z F_x + \psi_x]_{z=F(x)} = 0. \tag{12}$$

The problem is now well defined. The A_n in (8) must be found by requiring that the solution (6) satisfy the boundary condition (12). The magnitude of these coefficients is then related to the energy density of each Fourier mode, and thus to the associated energy flux of that mode. The energy density of a particular wave (Bretherton 1969) is the space–time average of

$$E = \tfrac{1}{2}\rho(|\mathbf{u}|^2 + N^2\zeta^2),$$

where ζ is the elevation of an isopycnal from its quiescent or rest position. Consequently, the value of the temporally, spatially averaged modal energy density is given by

$$\overline{E_n} = \frac{\omega lk}{(2\pi)^3}\int_0^{2\pi/\omega}\int_0^{2\pi/l}\int_0^{2\pi/k} E_n\,dx\,dz\,dt = \rho N^2 k^2 |A_n|^2/2\omega^2,$$

with the kinetic and potential energies being equal for these small amplitude waves. From (4), the average *rate* at which a particular mode transports energy vertically is

$$-\overline{E_n}\{N|k_n|\,l_n/(k_n^2 + l_n^2)^{\frac{3}{2}}\},$$

and the statement that energy must be conserved in the reflexion is thus written with the use of (8) by equating the incoming and scattered energy fluxes:

$$\sum_{n=-\infty}^{+\infty} |l_n(k+np)^3|\,|A_n|^2/[(k+np)^2 + l_n^2]^{\frac{3}{2}} = lk^3/(k^2+l^2)^{\frac{3}{2}}. \tag{13}$$

In the following section, we shall find the A_n and use (13) as a check on the accuracy and convergence of the calculation.

3. Method of solution

Substitution of (6)–(8) into the boundary condition (12) yields

$$(-lap\sin px+k)\exp(ila\cos px)$$
$$+\sum_{n=-\infty}^{+\infty}A_n[\Gamma^{-1}|k+np|\,ap\sin(px)+k+np]\exp(inpx)\exp(-i|l_n|\,a\cos px)=0, \tag{14}$$

where $$\Gamma=|k+np|/l_n=k/l=\cot\theta.$$

Clearly, functions with many different periodicities arise from products of terms like $\sin(px)\exp(inpx)\exp(-i|l_n|a\cos px)$. It is not possible to solve for the A_n using orthogonality properties of these periodic functions because they are not all harmonics of the same function. We shall therefore find the coefficients by a least-squares technique (Dugan 1973). If we put

$$f(x)=(lap\sin px-k)\exp(ila\cos px),$$

and

$$g_n(x)=[\Gamma^{-1}|k+np|\,ap\sin px+k+np]\exp(inpx)\exp(-i|l_n|a\cos px),$$

then (14) is equivalent to

$$F(x)=\sum_{n=-\infty}^{+\infty}A_ng_n(x). \tag{15}$$

Or, truncating the series, we have

$$f(x)\approx\sum_{n=-N}^{+N}A_ng_n(x). \tag{16}$$

At some point $x=x_i$, (16) will not in general be satisfied because it is an approximation to (15) containing only $2N+1$ terms. In fact, the error at the point $x=x_i$ is given by

$$d_i=f(x_i)-\sum_{n=-N}^{+N}A_ng_n(x_i).$$

We may solve for the coefficients of (16) by collocating at many points x_i and minimizing the sum of the squares of the errors by a judicious choice of the A_n. Since the sum of the squares of the errors is

$$\sum_{i=1}^{I}d_i^2=\sum_{i=1}^{I}\left[f(x_i)-\sum_{n=-N}^{N}A_ng_n(x_i)\right]^2,$$

we see that

$$\partial\left[\sum_{i=1}^{I}d_i^2\right]\Big/\partial A_m=\sum_{i=1}^{I}2\left[f(x_i)-\sum_{n=-N}^{N}A_ng_n(x_i)\right][-g_m(x_i)]=0. \tag{17}$$

If we presume uniform convergence, we may reverse the order of the sums and thus (17) becomes

$$\sum_{i=1}^{I}f(x_i)\,g_m(x_i)=\sum_{n=-N}^{+N}\sum_{i=1}^{I}A_ng_n(x_i)\,g_m(x_i),$$

which must be satisfied for $m=0,\pm1,\ldots,\pm N$. We now have $2N+1$ equations containing $2N+1$ variables. The variables are complex, and here this system is solved by using the method of pivotal condensation (Noble 1969).

Although any number of collocation points may be used, we shall use multiples of $2N+1$ (generally three or four times $2N+1$) because it is found that accuracy does not materially improve after that number. Furthermore, it is found that for most cases when $N \geqslant 9$ the coefficient $A_9 \ll A_0$ or $A_{\pm 1}$. To provide a more quantitative test of this suggested convergence, the r.m.s. error in the approximation (16) can be calculated in order to delineate the dependence upon the number of equations and the value of the wall slope. The r.m.s. error is approximated by

$$\epsilon = \left\{\frac{1}{J}\sum_{j=1}^{J}\left[f(x_j) - \sum_{n=-N}^{+N} A_n g_n(x_j)\right]^2\right\}^{\frac{1}{2}}, \tag{18}$$

where J is nominally taken to be $10(2N+1)$, or ten times the number of equations. In figure 1, ϵ is plotted as a function of the number of equations for several wall slopes. Here $p/k = 2$, $\theta = 60°$ and ap varies from 0·05 to 0·3. As might be expected, the case $ap = 0{\cdot}05$ seems to converge the most rapidly of all those shown, the error ϵ decreasing exponentially with the number of equations. On the other hand, it is obvious that, regardless of how many terms in (16) are used to describe the case $ap = 0{\cdot}3$, the sum can never converge. While the case $ap = 0{\cdot}05$ converges and $ap = 0{\cdot}3$ is clearly divergent, we are led to inquire regarding the behaviour of cases of intermediate ap, 0·2 and 0·25 say. For $ap = 0{\cdot}2$, ϵ continues to decrease as the number of equations increases; convergence seems assured, but no new insight is gained as the number of equations is increased. For $ap = 0{\cdot}25$ however, the error begins to increase with the thirty-first term in (16); this case is clearly asymptotic, and the best approximation to the answer is obtained by retaining only 29 terms.

The series behaviour exhibited in figure 1 is typical of the properties of this solution. For any given ap and p/k, the r.m.s. error ϵ is a function of the number of equations. This sequence of final values $\epsilon = \epsilon(2N+1)$ is observed to possess the character of a series of partial sums which is asymptotic. For slopes below a certain value, there exists no practical way of distinguishing whether the series is asymptotic or convergent, because of the number of terms required to do so. Indeed, because this number is frequently too large for the machine, the distinction is moot. Our main concern will therefore be the accuracy of the series representation of the solution and the conservation of energy in the reflexion process.

In the case of divergence of the series (15), the moduli of the coefficients A_n – a measure of the reflected energy flux – are seen to remain the same or to increase as the number of equations is increased. This is clearly incorrect as it implies that energy is being created in the reflexion process. With the use of (13), the ratio of reflected to incoming energy flux may be expressed as

$$C = \frac{\sum_{n=-N}^{+N} |l_n(k+np)^3|\,|A_n|^2[(k+np)^2+l_n^2]^{-\frac{3}{2}}}{lk^3(k^2+l^2)^{-\frac{3}{2}}}, \tag{19}$$

and when (14) converges, C is identically unity.† If the series diverges, C is found to be greater than $1{\cdot}0 \pm 10^{-8}$, and, in fact, the calculation of $\Delta C = |C - 1{\cdot}0|$

† To within a deviation of 10^{-8}, the accuracy to which these calculations were performed.

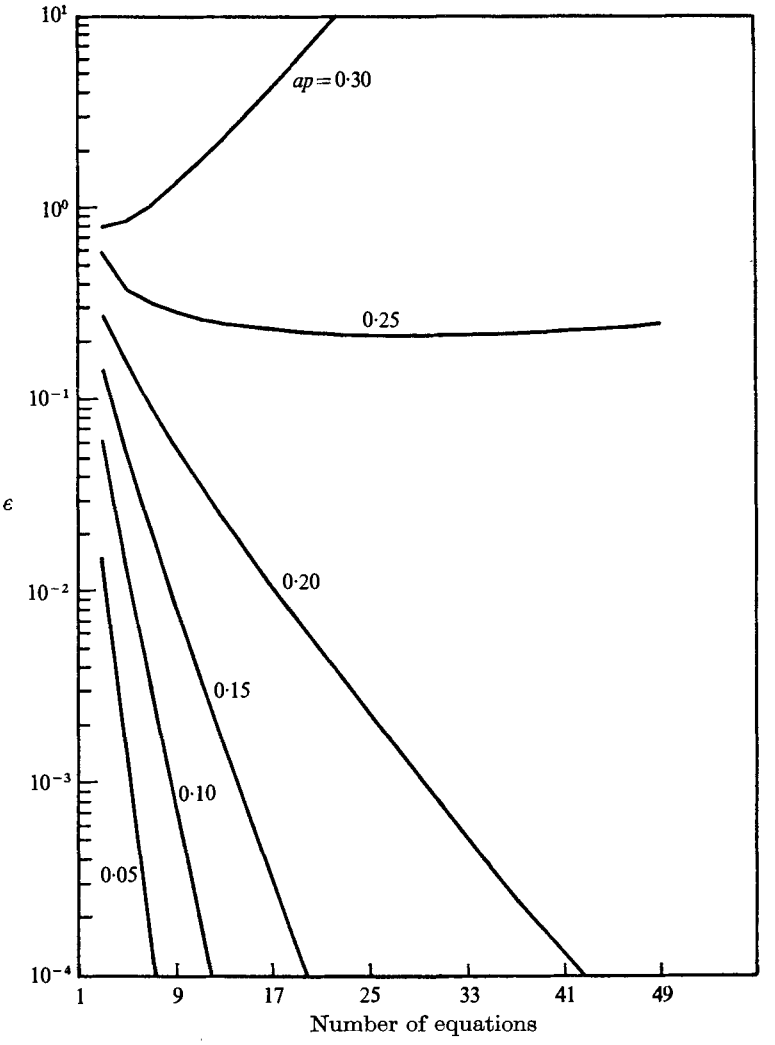

FIGURE 1. The r.m.s. error as a function of the number of equations for several wall slopes ap. Here $p/k = 2{\cdot}0$, $\theta = 60°$, and the ratio of the number of collocation points to the number of equations is four. The points at which the r.m.s. error is evaluated are evenly spaced along $0 \leqslant x \leqslant 2\pi/p$, and they number ten times the number of equations.

is found to be a much more sensitive indicator of when the series first begins to diverge, as opposed to monitoring ϵ for increasing ap or θ.

As an example of the convergence properties of this series, we plot in figure 2 regions of convergence and divergence in the ap, θ plane. The region of divergence is shaded. The line $\theta = \cot^{-1}(ap)$ is shown in this figure also. For all θ above this line, the maximum slope ap of the wall is greater than $\cot\theta$, the slope of the group velocity wave rays. In this region, we should expect divergence because the solution is not valid everywhere above the corrugation. Specifically, there are some regions within the troughs of the corrugations which are sheltered, i.e. hidden from the source which propagates energy along an incoming wave ray.

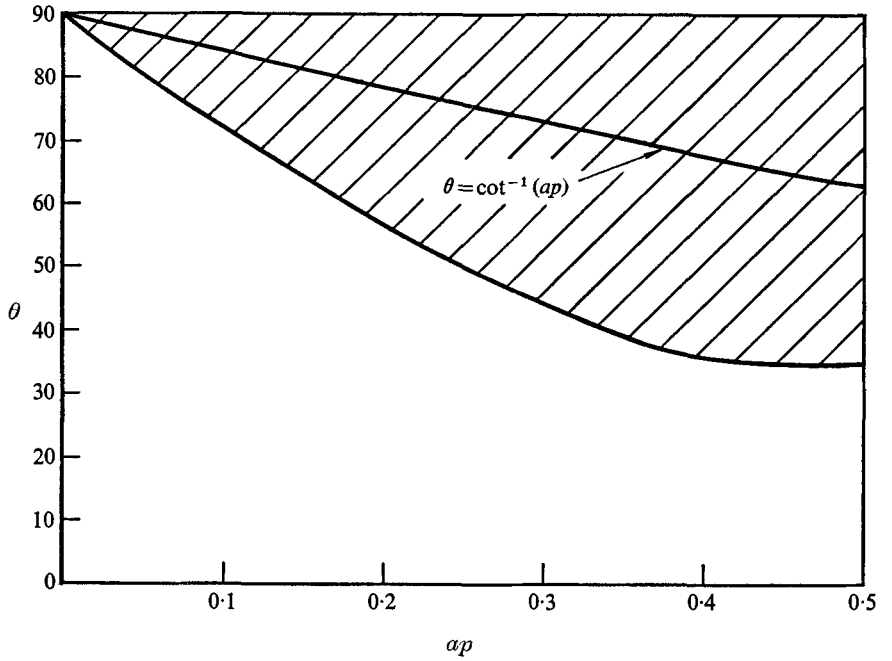

FIGURE 2. A typical plot of the convergent/divergent character of the series when Rayleigh's method is applied to this problem. The region of divergence is shaded and the line $\theta = \cot^{-1} ap$ is plotted; above this line the group velocity wave rays are incident at such a shallow angle that they are sheltered by a wall of sufficiently large slope. $p/k = 0{\cdot}445$.

Since shadowing cannot account for all of the divergent region, some additional unknown phenomenon must limit the region of validity of the series solution.

In the following section, the implications of the solution for the forward- and back-scattered energy fluxes are discussed. Comparison with the linear results of Baines (1971) is made and, to facilitate this comparison, we point out that his variables $k_1 c$, l, d and c correspond to k, p, a and $\cot\theta$ in the present work. It also seems appropriate to mention in this regard that his scattered fields conserve the energy of the incoming wave to $O(a^2k^2/\cot^2\theta)$.

4. Properties of the solution

As the slope of the wall corrugations is increased, one would expect the reflected energy to exhibit less of a specular character. That is, progressively more energy should appear in modes for which $n \neq 0$ in (16). In figure 3, we see that this trend is in fact quite pronounced, with the $n = \pm 1$ modes having higher coefficient moduli than the specularly reflected mode ($n = 0$) beyond a wall slope of about $\frac{1}{3}$. For this particular case, $\theta = 45°$ and $k/p \approx 2{\cdot}25$, so that, according to (9), only modes for which $n \leqslant -3$ will be back-scattered. Coincidentally, the $n = -3$, -4 modes lie in the range $|A_n| \leqslant 10^{-2}$ and so do not appear in this figure.

A better quantitative impression of the redistribution of energy from the

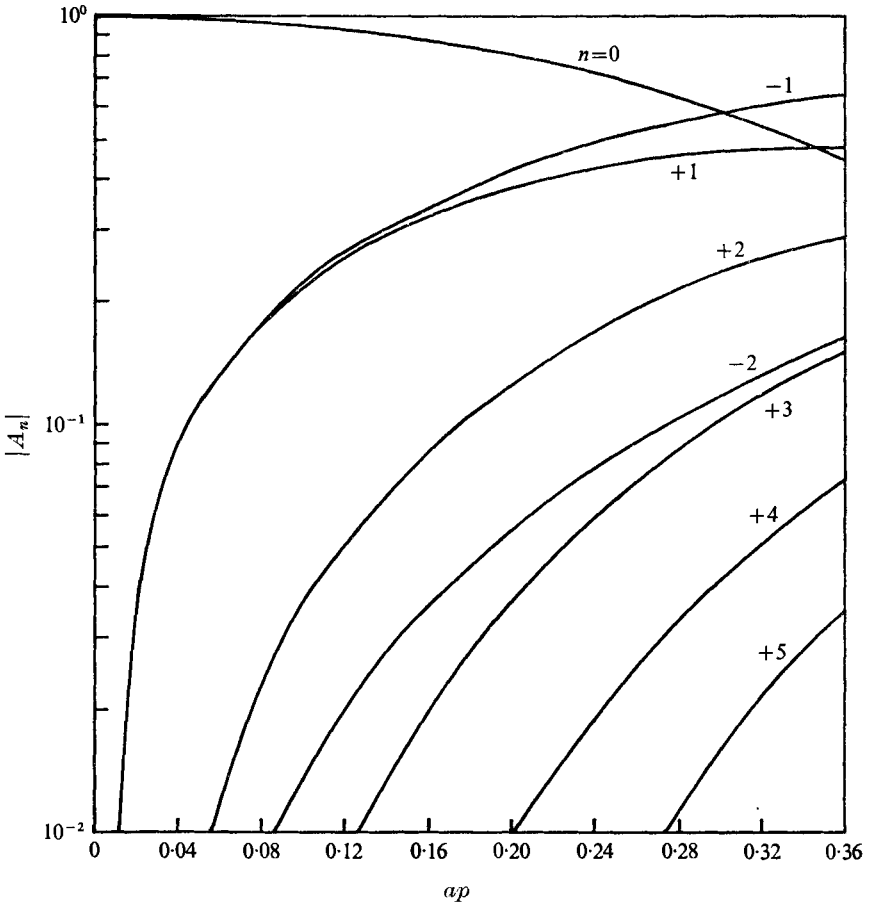

FIGURE 3. The moduli of the A_n for $-2 \leqslant n \leqslant +5$ as a function of wall slope. $\theta = 45°$, the number of equations is 25, and the number of collocation points per wall wavelength is 75. Because $k = 2{\cdot}25p$, the lowest back-scattered mode corresponds to $n = -3$, and $|A_{-3}| < 10^{-2}$.

specularly reflected mode to other modes as ap is increased may be obtained by plotting the ratio of specular energy flux to total incoming energy flux r_s and also the ratio of back-scattered to forward-scattered energy flux r_b. These are plotted as a function of ap for several angles in figures 4(a) and (b) respectively. As the wall slope is increased for a given number of equations, the accuracy that can be maintained with only 25 equations is decreased. The r.m.s. error defined in (18) increases markedly and ΔC grows to the order of 10^{-7}. In this case, the curve on the graph is terminated when ΔC becomes this large; however, ϵ is no more than the order of a per cent or so, and the exact value is noted in the figure caption. The work of Baines indicates that

$$r_s \simeq \left\{1 - \left[\frac{ap}{(p/k)\cot\theta}\right]^2\right\}^2, \quad \frac{ap}{(p/k)\cot\theta} \ll 1,$$

and this is shown in figure 4(a) as a dashed line. In spite of the fact that only three terms are retained in this linear solution, the agreement with the present

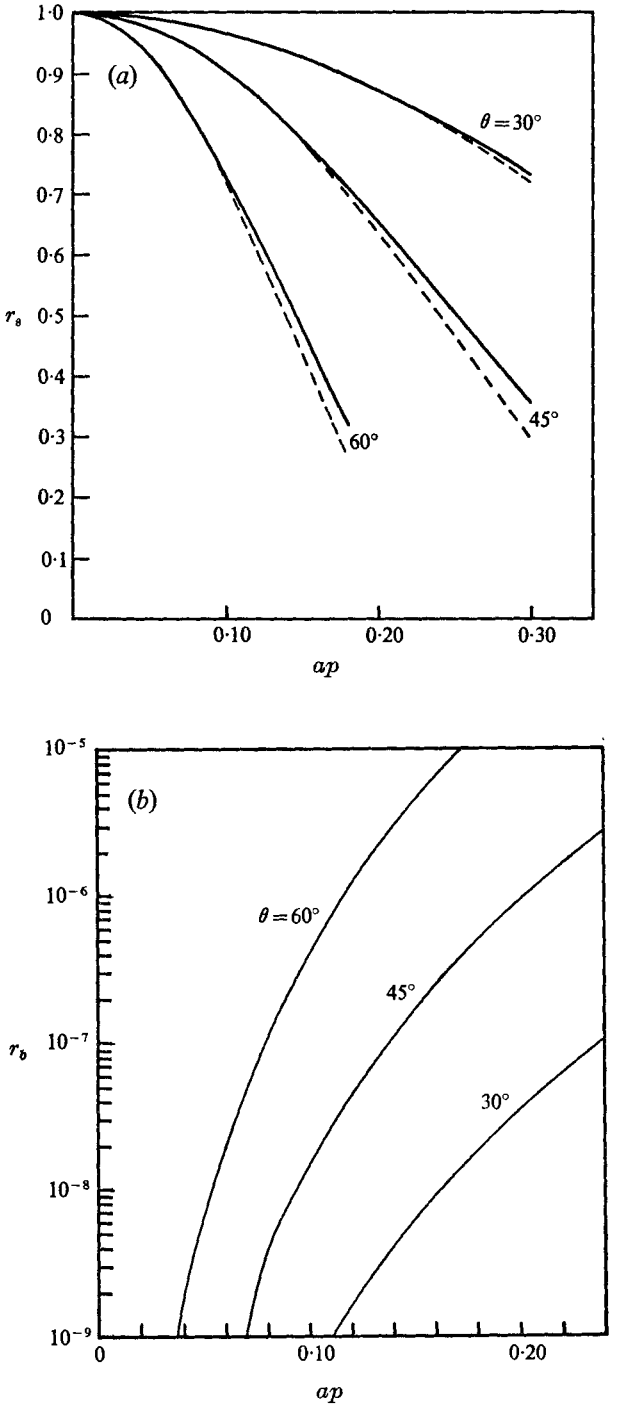

FIGURES 4(*a*, *b*). For legend see facing page.

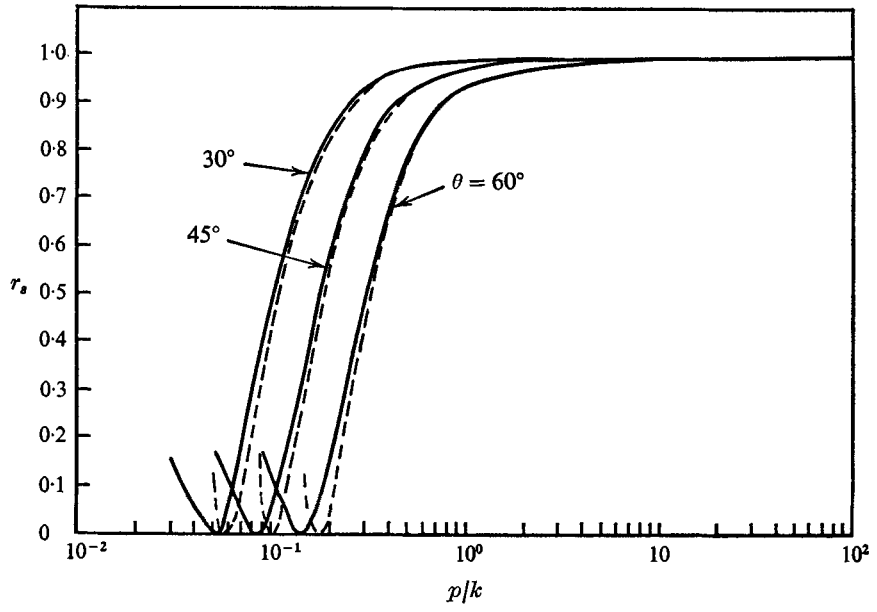

FIGURE 5. A plot of the ratio r_s of the specularly reflected to incoming energy flux as a function of p/k for $\theta = 30°$, 45° and 60° (solid lines). $ap = 0{\cdot}1$ and k is varied. The number of equations is 25 and there are 100 collocation points per wavelength. For the lowest value of p/k plotted, the curves are terminated when ΔC is of the order of 10^{-7} and the r.m.s. error grows to 0·4%. The dashed lines are the results of Baines (1971).

25-term case is excellent for most of the range of ap. No similar comparison can be made in figure 4(*b*) because, for the value of p/k employed here, the lowest-order back-scattered mode corresponds to $n = -3$, which would require the retention of seven terms to effect a comparison.

In the limit of large p/k, the horizontal wavelength of the internal wave is large with respect to the wall corrugation wavelength. This is the 'smooth surface' reflexion limit and, in this case, we should expect almost all of the energy to be specularly reflected. This is the observed behaviour of course, but the surprising result revealed in figure 5 is that of the order of 95% of the incoming energy flux is reflected in the specular mode (for $\theta = 30°$, 45°, 60°) provided only that $p \gtrsim k$. In the limit of small p/k, a substantial amount of reflected energy is transferred out of the specularly reflected mode and this is evident from the figure. Although we cannot explain the existence of the windows in the vicinity

FIGURE 4. (*a*) The ratio r_s of specularly reflected to total incoming energy flux for $\theta = 30°$, 45° and 60° as a function of wall slope (solid lines). For the largest value of ap plotted, ΔC has grown to $O(10^{-7})$ and the r.m.s. errors are less than $1{\cdot}3 \times 10^{-4}$%, 1·0% and 2·0% respectively. $p/k = 0{\cdot}445$; there are 25 equations and 100 collocation points per wall wavelength. The dashed lines are the results of Baines (1971). (*b*) The ratio r_b of back-scattered to forward-scattered energy flux for $\theta = 30°$, 45° and 60°. At the highest value of ap on each curve, ΔC is $O(10^{-7})$ and the r.m.s. errors are less than 5×10^{-6}%, 0·03% and 0·25% respectively. The graphs are plotted for $p/k = 0{\cdot}445$, while the number of equations is 25 and there are 100 collocation points per wall corrugation wavelength.

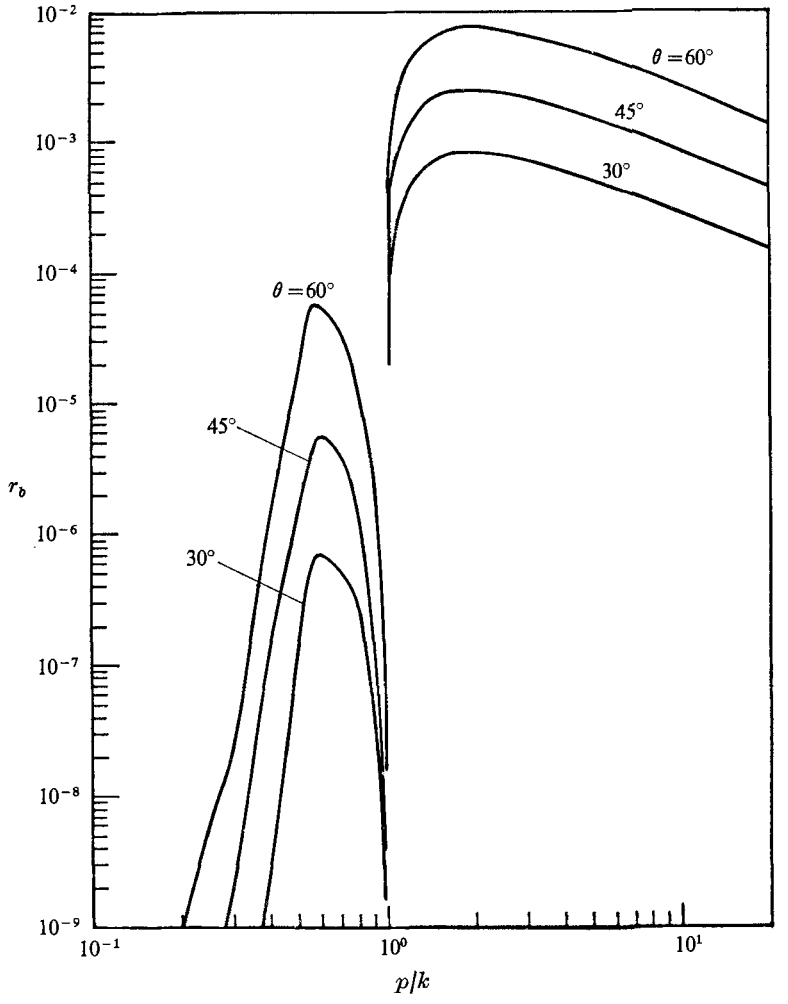

FIGURE 6. The ratio r_b of back-scattered to forward-scattered energy flux as a function of p/k for $\theta = 30°$, 45° and 60°. The wall slope $ap = 0{\cdot}1$ and k is varied. There are 100 collocation points, 25 equations, and $\Delta C < 10^{-7}$. Baines' (1971) result agrees perfectly with those of the present study when $p/k > 1$, but yields no back-scattered flux when $p/k < 1$.

of $p/k = 0{\cdot}1$, we note that the curve is a smoothly varying function of p/k. Baines' three-term linearized results for r_s (also given in figure 4a) are shown as dashed lines. The agreement is excellent over much of the range of p/k, and his expression also yields a value of p/k for which no energy appears in the specular mode.

From (9), we see that $k_n = 0$ whenever $n = -p/k$, and this corresponds to a vertically propagating wave. As a particular $k_n \to 0$, however, the A_n associated with it vanishes also, the energy appearing in other modes. The smoothness of the curve through these points is an indication of the fact that no singularities arise when $k_n = 0$. In figure 6, the ratio of back-scattered to forward-scattered

energy flux is also shown as a function of p/k. For all angles ($\theta = 30°, 45°$ and $60°$) it is found that very little energy is back-reflected when $p \simeq k$. Moreover, the peaks of the branches of the curves for $p/k < 1$ are of the order of 10^{-3} to 10^{-2} smaller than the peaks of the corresponding branches for $p/k > 1$. We may conclude, however, that, for the angles shown, virtually no energy is back-scattered when the horizontal wavelength of the incoming wave is less than the scale length of the wall. Baines' results can be manipulated to yield

$$r_b = \begin{cases} \dfrac{p/k - 1}{\left[\left(\dfrac{p}{k}\right)\dfrac{\cot\theta}{ap} - \dfrac{ap}{\cot\theta}\right]^2 + (p/k + 1)}, & p > k, \\ 0, \quad p < k. \end{cases}$$

It is interesting to note that here the linear calculation gives a result which plots directly over the numerically obtained curve in figure 6 when $p/k > 1$, while failing to predict any back-scattering when $p/k < 1$.

5. Conclusion

We have demonstrated that an extension of Rayleigh's method using a variational technique is applicable to the problem of internal wave reflexion from a sinusoidally corrugated wall with large slope; and that, for many wall slopes and angles of wave incidence, the series will converge. These calculations have been verified by computing the energy flux reflecting from the wall and observing that it balances the incoming flux. In so doing, we note that, in all of the cases tested, of the order of 90 % of the incoming energy is reflected from the wall in the specular mode as long as the horizontal internal wavelength is greater than the corrugation wavelength of the wall. Moreover, the back-scattered energy flux is never more than a per cent or so of the forward-scattered flux for all of these cases.

Perhaps the most significant result of this paper is that the linearized reflexion theory of Baines (1971) is surprisingly accurate almost up to the limits of convergence of the series when used to predict forward-scattered energy flux. Care must be exercised when interpreting the results of the linear theory as regards back-scattered energy, however.

REFERENCES

BAINES, P. G. 1971 The reflexion of internal/inertial waves from bumpy surfaces. *J. Fluid Mech.* **46**, 273.

BELL, T. H. 1975 Topographically generated internal waves in the open ocean. *J. Geophys. Res.* **80**, 320.

BRETHERTON, F. P. 1969 Momentum transport by gravity waves. *Quart. J. Roy. Met. Soc.* **95**, 213.

DUGAN, J. P. 1973 A variational method for scattering by an arbitrarily shaped obstacle. In *Variational Methods in Engineering, Proc. Int. Conf. Var. Meth., Southampton*, 1972, pp. 11/49–11/58. Southampton University Press, Surrey.

LEE, C. Y. & BEARDSLEY, R. C. 1974 The generation of long nonlinear internal waves in a weakly stratified shear flow. *J. Geophys. Res.* **79**, 453.

MIED, R. P. & DUGAN, J. P. 1974 Internal gravity wave reflection by a layered density anomaly. *J. Phys. Ocean.* **4**, 493.

MIED, R. P. & DUGAN, J. P. 1975 Internal wave reflection by a velocity shear and density anomaly. *J. Phys. Ocean.* **5**, 279.

NOBLE, B. 1969 *Applied Linear Algebra.* Prentice-Hall.

PHILLIPS, O. M. 1966 *The Dynamics of the Upper Ocean.* Cambridge University Press.

RAYLEIGH, LORD 1945 *The Theory of Sound*, vol. II. Dover.